The Design of 3D Laser Range Finder for Robot Navigation and Mapping in Industrial Environment with Point Clouds Preprocessing

Petr Olivka[1(✉)], Milan Mihola[2], Petr Novák[2], Tomáš Kot[2], and Ján Babjak[2]

[1] Department of Computer Science, FEECS, VŠB – Technical University of Ostrava, Ostrava, Czech Republic
petr.olivka@vsb.cz

[2] Department of Robotics, FME, VŠB – Technical University of Ostrava, Ostrava, Czech Republic
{milan.mihola,petr.novak,tomas.kot,jan.babjak}@vsb.cz
http://www.vsb.cz

Abstract. This article describes the design of 3D Laser range finder (LRF) for industrial and mine environment. The 3D LRF is designed for usage on middle size robots and can be used for environment mapping and navigation. The design reflects heavy and dirty working conditions in industrial environment and it is equipped by own methane sensor for usage in mine. The process of design started with definition of requirements, follows by dynamic analysis and selection of suitable parts. The housing is designed from stainless steel and it encloses all electrical and mechanical components. The internal control unit is designed to suit modern trends of fog computing. It is equipped with four cores ARM CPU and IMU and it is able to preprocess the acquired point clouds in real time.

Keywords: Robot · Mapping · Navigation · Laser range finder · Fog computing · Point clouds

1 Introduction

The navigation and mapping subsystem of mobile robot is integral part of a robot control system. Many various methods are used in a practice and their algorithms depend on used type of sensors. One of the most suitable sensor for navigation and mapping is a laser range finder (LRF).

Nowadays on the market many types of 3D LRF are available. One of the most known 3D LRF producer is Velodyne. Its products are very often used for autonomous control of cars. The Velodyne Lidar HDL-64E is visible in Fig. 1. This lidar has the horizontal field of view (FOV) 360° but the vertical FOV is only 27°. Its measurement range is up to 120 m and power consumption 60W. These technical parameters are suitable for the outdoor usage, especially in the traffic environment, but disadvantaging it for indoor usage. The high power consumption is limiting factor for power supply from batteries. The narrow vertical

J. Hodicky (Ed.): MESAS 2016, LNCS 9991, pp. 371–383, 2016.
DOI: 10.1007/978-3-319-47605-6_30

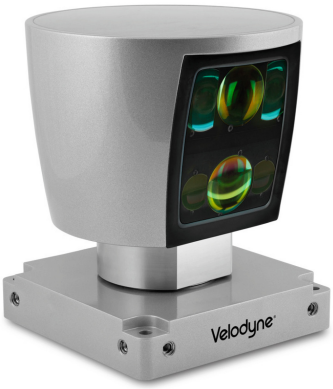

Fig. 1. Velodyne LIDAR HDL-64E [9]

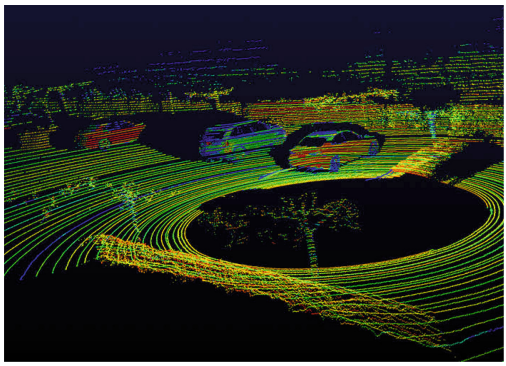

Fig. 2. Raw data from HDL-64E [9]

FOV allows to fully recognize obstacles with size of adult person from distance approximately 4 m. In Fig. 2 is an example of data captured by HDL-64E and there is visible that the first points of ground are detected by this lidar at distance about 3 m. Any large obstacles at closer range can be only detected, but not recognized. Moreover the overall coverage of a surrounding environment is only 15 %. The large blind space is above and below this lidar. The last but not least disadvantage is the very high price of this lidar – around $70000. The smaller version of Velodyne lidar HDL-32E costs around $29000.

On the opposite side to professional industrial 3D LRF devices, solutions for office and home usage are available. The examples are Kinect, visible in Fig. 3 and Xtion showed in Fig. 4. These devices are mass-produced, therefore they are cheap, but they are unusable for industrial applications.

The high price of high-quality 3D LRFs is still the main limiting factor for their wider use in industrial applications.

Fig. 3. Kinect [http://www.microsoft.com]

Fig. 4. Xtion PRO LIVE [http://www.asus.com]

A number of designers are therefore thinking about cheaper design. The market offers the an alternative – the 2D LRF. There are two well-known producers of 2D LRF on the market with relative wide range of product lines – Sick and Hokuyo.

Fig. 5. First know design of 3D LRF with servo [8]

Fig. 6. Zebedee design of 3D LRF with 2D LRF mounted on spring [1]

For the 2D LRF usage in 3D applications is only necessary to add the third dimension. Probably the first documented design of 2D LRF used for 3D measuring, introduced in 2009, is visible in Fig. 5. The main weakness of this design is the mounting of the carrier directly to the servo. The servo is not able to capture all inertial forces of the mounted LRF and this design will damage very soon the gears and their bearings inside the servo.

The different approach to 3D LRF design is shown in Fig. 6 and this design was introduced in [1]. The 2D LRF is mounted on a spring and the third spatial dimension is added by swinging. This design has two main disadvantages. At first it is the requirement of manual swinging which causes the irregular coverage of environment. The second disadvantage is necessity of using IMU, which is mounted below the LRF, and the perfect time synchronization of IMU and LRF.

The design with LRF mounted on the horizontal axis was presented in [2] and its design is shown in Fig. 7. Nevertheless this design has limited rear visibility.

The own design of 3D LRF was developed in our lab, inspired by [8]. The 2D LRF Hokuyo URG-04LX is mounted on a step motor which captures all inertial forces of the carrier and LRF in their ball bearings. The vertical orientation of the rotatable axis guarantees the same views to all sides and this laser is able to measure 66 % of space. The blind space is under this 3D LRF. The overall design of 3D LRF is depicted in Fig. 8.

The first version of 3D LRF required a special microstepping unit [4], but the latest design uses a step motor with 400 physical steps per revolution and a common circuit DRV8825 is used for the control. The main control unit is composed of Raspberry Pi 2 computer and real-time control circuit is realized by Arduino Nano. For reliable usage of the short range LRF Hokuyo, it is necessary to calibrate it. The calibration process is described in [6].

This 3D LRF was successfully used in a few applications and the gained experiences were used for design of new industrial version of 3D LRF, introduced herein below.

Fig. 7. LRF mounted on the horizontally oriented axis [2]

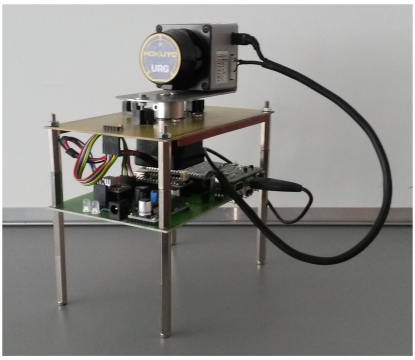

Fig. 8. LRF Hokuyo URG-04LX mounted on the vertically oriented step motor

2 Desired Parameters of 3D LRF Design for the Industrial Environment

For the proper design of industrial 3D LRF it is necessary to define a set of parameters, which is required for good and perspective design. The main requirements to 2D LRF are: measured distance up to 20 m, frequency of scanning at least 25 Hz, measuring angular range at least 240°, data interface USB or Ethernet for fast data transfer and power supply and data line in one cable. Because it is planned to use this 3D LRF even in mine, the good black surface detection must be preferred too.

For the autonomous usage the unit must be equipped with its own power supply in the form of batteries. The dust and water proof design is expected naturally. Additionally, for the potential underground work it will be necessary equip the device with methane sensor.

Most of the required parameters are related to the main part: the 2D LRF. On the market are available many products in product lines of Hokuyo and Sick producers. But only a few of them fulfill the required parameters. The main problem is the detection of black surface. This requirement considerably narrows the assortment of suitable LRF.

Both the producers mentioned above have in their product lines only one LRF designed for black surface. But only the Sick LRF was available from our supplier and therefore we had to use it.

The compliant scanner is Sick LMS111. Its main technical characteristics can be found in [10].

The selection of the most important parameters: dimensions 105 × 102 × 162 mm, weight 1.1 kg, scanning frequency 25 or 50 Hz, resolution 0.5 or 0.25°, measuring angular range 270° and operating range up to 20 m. Power consumption is 8 W, enclosure IP67 and communication interface Ethernet 10/100Mbit/s, systematic error of measuring is ±30 mm.

The power and the Ethernet cables of the LMS111 are from production separated. But there is an easy possibility to integrate them together in the PoE (Power over Ethernet) form.

The first testing of the LMS111 discovered an impossible combination of measurement resolution and scanning frequency. The resolution 0.25° cannot be used at frequency 50 Hz. This problem was not explained in the documentation, neither by the supplier. Therefore at 50 Hz the only possible resolution is 0.5°.

The design of the positioning unit for the relatively large and heavy LMS111 will be described in following sections.

3 Dynamic Analysis of Positioning Unit Design

It is not possible to mount the LMS111 in such an easy way as it was shown in Fig. 8. This scanner is relatively heavy and it is not possible to mount it directly on the step motor. Moreover the step motor is not suitable for design of a battery-powered device because of its high and continuous power consumption.

The rotatable mounting of the LMS111 has to be designed to capture all inertial forces that may occur during movement. Therefore the shaft for the carrier with the LMS111 is mounted in two ball bearings inside a sleeve. The overall design is depicted in Fig. 9. The LSM111 is mounted in its centroid for the maximal elimination of inertial forces. The centroid position is not listed in technical documentation, it had to be found experimentally.

For the proper selection of a rotating actuator it is necessary to perform the dynamic analysis of the designed rotatable mounting with the LMS111. But the design is not sufficient for analysis. Some additional information is needed.

The first unknown parameter is the rotating motion sequence. The theoretical course of the angular velocity between two positions is visible in Fig. 10. Here

Fig. 9. Rotatable mounting of LMS111 on axis with pair of ball bearings inside sleeve

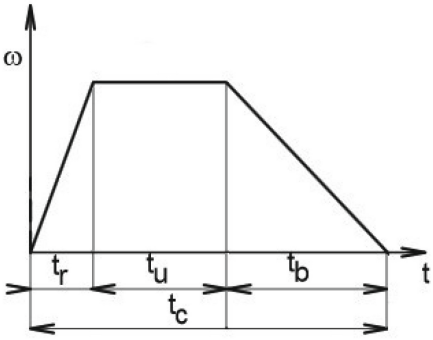

Fig. 10. Course of angular velocity between two angular positions [3]

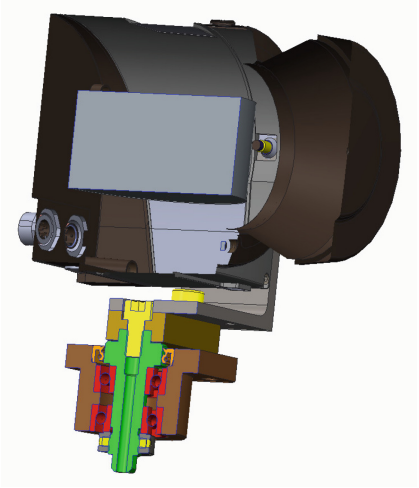

Fig. 11. Valve model of LMS111 for dynamic analysis

it is necessary to know the time t_c of rotation and angle between two positions. The time can be easily computed from the known parameters of the LMS111. The highest frequency of scanning is 50 Hz. The time period for this frequency is $t_1 = 20$ ms. The angular range of scanning is 270° and blind space is the rest of a turn, which is 90°.

The LMS111 has to be rotated in the blind space, that is one quarter of t_1. Thus the time of rotation t_c should be 5 ms or less.

The angle between two scanning position, during the LMS111 rotation, should be the same as the LMS111 resolution. The maximal angle is 0.5°. Now the time t_c and angular distance between two scanning position are known.

The penultimate unknown parameter for dynamic analysis is the LMS111 mass moment of inertia. This information is not available even in 3D model of the LMS111 supplied by its producer. Thus for the simulation the LMS111 can be replaced by a virtual valve with the similar dimensions as the LMS111 metal body and with the same weight. The virtual valve model is visible in Fig. 11.

The last unknown parameter of rotatable mounting showed in Fig. 9 is the friction torque between the radial shaft seal and the shaft itself. According to the known material of the proposed seal and the shaft surface quality the friction torque 1000 N·mm can be used.

The PTC Creo Parametric software [13] was used for the dynamic analysis. This software automatically computes every necessary moment of inertia of all parts from the 3D model. The additional input parameters are the course of movement, depicted in Fig. 10, and the angle between two positions, described above. The whole time t_c of the movement can be divided to three phases: the time of acceleration t_r, the time of constant velocity rotation t_u and the time of deceleration t_b.

The result of dynamic analysis is shown in Figs. 12 and 13.

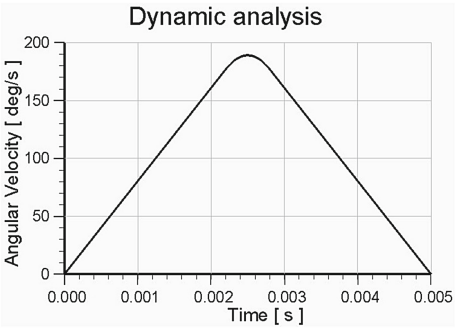

Fig. 12. Course of angular velocity

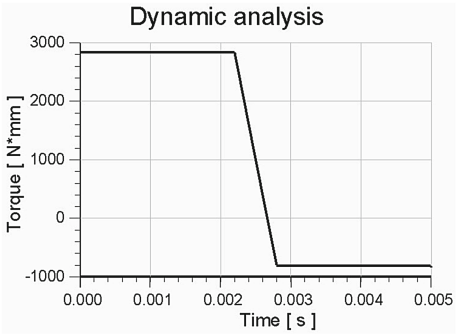

Fig. 13. Course of required torque

The course of angular velocity is depicted in Fig. 12. This course corresponds to the theoretical course in Fig. 10. Because of the very small angle between two positions the phase with constant velocity is missing. The angular movement contains only the acceleration and deceleration phases.

The course of the torque computed by Creo is visible in Fig. 13. This course corresponds to the theoretical angular velocity with a short phase of acceleration and a short deceleration. The difference between the acceleration and deceleration torque is caused by the internal friction in the rotatable mounting.

The dynamic analysis found two main important parameters for actuator selection. The maximal required angular velocity is 200°/s and the maximal torque is 3000 N·mm.

The market offers many suitable rotating actuators which fulfill the required parameters for the design proposed earlier. The additional parameters for selection should be: small dimensions, low power consumption, easy control, good angular position control and the same power supply voltage as the LMS111.

The servo Dynamixel MX-64R was selected as a suitable actuator. The list of its technical parameters is in the e-manual or data sheet [11]. The range of power supply is 12–14.8 V, maximum current 4 A, quiescent (standby) current 100 mA, communication interface RS-485, maximum torque 6000 N·mm, angular resolution 4096 steps per turn guaranteed by inner magnetic sensor, maximum rotating speed 63 rpm and weight only 126 g.

4 Positioning Unit Design

The design of the only moving part of the positioning unit was depicted in Fig. 9. For the overall design it is at first necessary to organize spatially all the internal parts into the smallest volume, while preserving enough manipulation space for the assembly process.

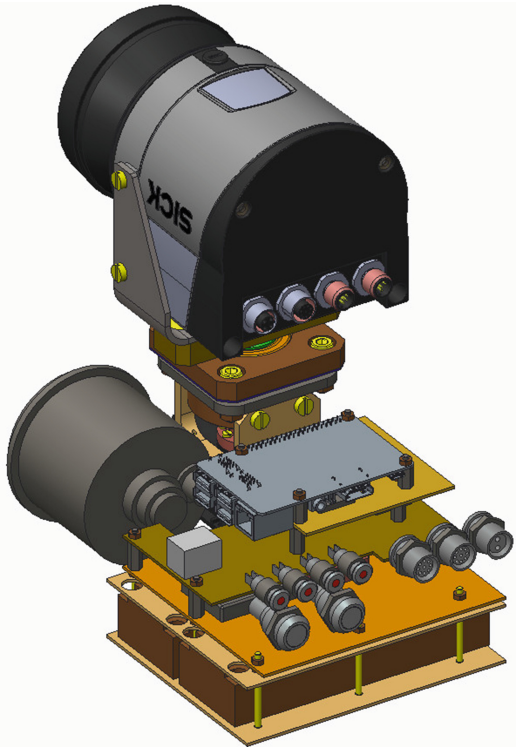

Fig. 14. Arrangement of all internal parts of positional unit

The proposed internal arrangement is depicted in Fig. 14. There are visible the four largest components: the not-yet-mentioned methane sensor SC-CH4 [12], the rotatable mounting with the servo and two batteries on the bottom. On the top is the LMS111, but it will be outside the positioning unit. The rest of the space is occupied by the electronic equipment, switches, LEDs and connectors.

All parts will be encapsulated in a metal housing. The overall design of this housing is visible in Figs. 15 and 16.

The housing is composed of two parts: bottom pan and top lid. These two parts are assembled together by 16 screws and the sleeve is mounted on the lid by 4 screws.

The first prototype of 3D LRF was made using rapid prototyping – printed on a 3D printer from polycarbonate. On this prototype the functionality and interoperability of all parts were verified. Subsequently the final prototype was completely made from stainless steel. The overall view of the welded prototype is visible in Figs. 17 and 18.

Fig. 15. Overall design of 3D LRF

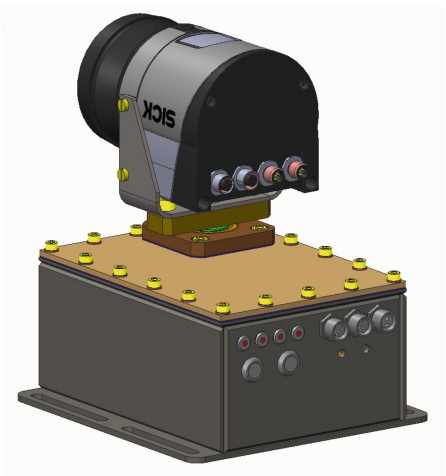

Fig. 16. Overall design of 3D LRF

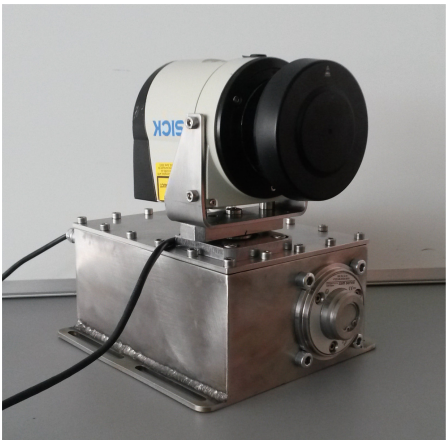

Fig. 17. Welded prototype of 3D LRF

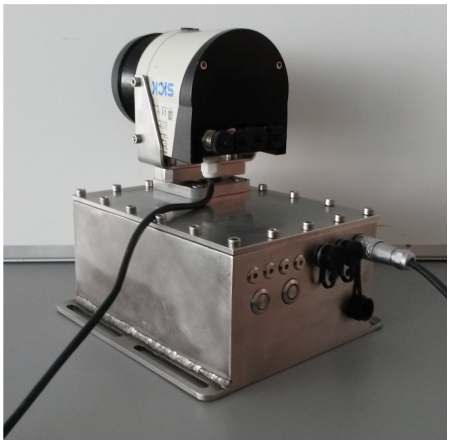

Fig. 18. Welded prototype of 3D LRF

5 Control System Unit of 3D LRF

The overall block diagram of the 3D LRF control system is depicted in Fig. 19. It is clear from this figure that the control system is relatively complex.

In Fig. 19 all parts of the control system are divided to two group separated by the horizontal dotted line. On the bottom of this diagram are power parts and above them are the control parts. The thicker solid lines represents the power supply from batteries. The thinner solid lines represent the 5 V power supply. This lower voltage power supply is generated by a DC/DC converter. All dashed lines denote data lines for communication. All parts in the diagram are marked according to their type or purpose.

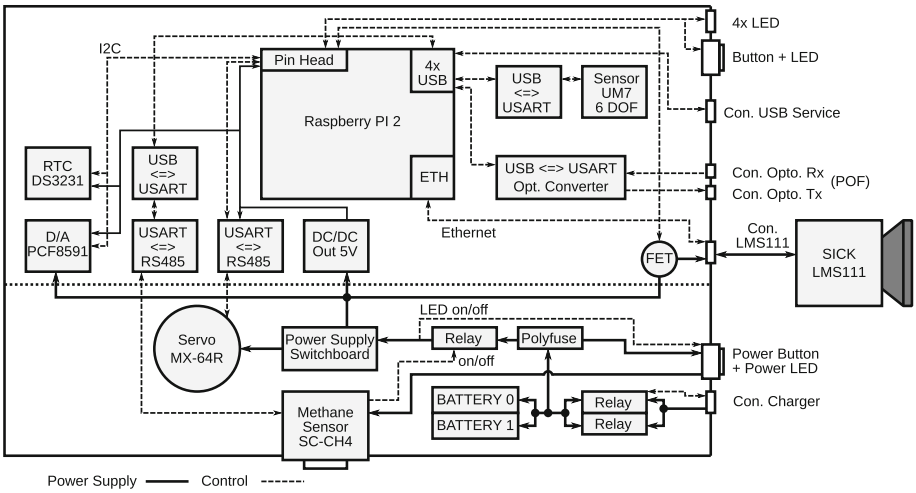

Fig. 19. Diagram of control system inside 3D LRF

The main control node is the SoC computer Raspberry Pi 2. This computer contains 4 ARM cores operating at frequency 1 GHz, 1 GB of DRAM memory, Ethernet 100 Mbit/s, 4 USB connectors, HDMI and a pin head. The pin head allows to connect devices with USART, SPI or I^2C interface. It contains also a few GPIO pins.

The power supply of the servo MX-64R is connected directly to batteries. Its internal control unit allows to switch the servo on and off and set current limit.

The interconnection between the LMS111 and the positioning unit is realized by a single cable with PoE, see Fig. 18. The power of the LMS111 has to be controlled by a power transistor.

Three USB interfaces are used for communication with three independent devices and the fourth USB interface is dedicated for service and diagnostic purposes.

The positional sensor UM7 detects inclination of the whole 3D LRF. The internal control unit of this sensor has implemented a Kalman filter.

The communication with another system is realized by Plastic Optical Fiber (POF) to achieve fully galvanic insulation between the connected systems and the POF guarantees safe functioning in a mine environment. This communication is also required for the exploration mobile robot [5].

6 Measuring Process and Captured Data Preprocessing

The measuring process will be described now. The LMS111 measures in a vertical plane with frequency 50 Hz. The resolution of this measuring is 0.5° in range 270°. The blind gap 90° is used for horizontal rotation of the LMS111 to a new position. This small rotation corresponds with LMS111 resolution and it is also 0.5°. This measuring process is repeated until the whole environment around the device

is captured, which occurs after half a horizontal revolution of the LMS111. The measuring process is in detail described in [6].

The measurement precision is derived from technical parameters of the LMS111 [10]. Because of measurement in rotating vertical plane the 3D LRF has the same precision in the horizontal and vertical direction. As was mentioned herein above, the precision is ±30 mm.

The required time for one measuring t_s can be computed from the known parameters by the following formula:

$$t_s = 180/(f_s \cdot \alpha_r) = 180/(50 * 0.5) = 7.2 \quad [\text{s}], \tag{1}$$

where f_s is scanning frequency and α_r is horizontal angular resolution. It is also possible to measure with resolution 0.25° in both axes, but the LMS111 must be slowed down to scanning frequency 25 Hz and the resulting time of one measuring will be 28.8 s.

The main computer inside the 3D LRF has to control many devices. Even so, it still has a sufficient surplus computing power (4 cores) which can be used for preprocessing of captured data in real time. This preprocessing performs a few successive tasks:

- Estimation of physical measuring ability of the LMS111. It depends on quality of the surface and its reflection.
- Detection of weak points and their removal.
- Detection and removal of outliers.
- Evaluation of information from the positioning sensor UM7 and compensation of measured data to the proper horizontal position.
- Transformation of captured data from spherical to Cartesian coordinate system.

After the preprocessing the data are passed to the main control system of the robot, which uses the 3D LRF. This principle, when cooperating systems perform data preprocessing and then they are passing data with increased value, is nowadays called “fog computing”. In practise it is a principle of computing power distribution between cooperating systems. The result is easier usage of data in the system which requested these data. For the testing is nowadays used the earlier developed control system for mobile robot [7].

7 3D LRF Testing

The testing of new industrial prototype was performed at first in a laboratory and then in a real underground environment in Gliwice (Poland) in the coal mine Queen Luiza. Because we tested carefully the functionality of the proposed 3D LRF design on the previous polycarbonate prototype, the final welded stainless steel industrial prototype was working well without problems.

Up to one hundred point clouds in 200 m long corridor were captured in the coal mine. All point clouds were automatically compensated to proper horizontal position and every point cloud was filtered during preprocessing. One example

Fig. 20. Underground corridor of the coal mine Queen Luiza

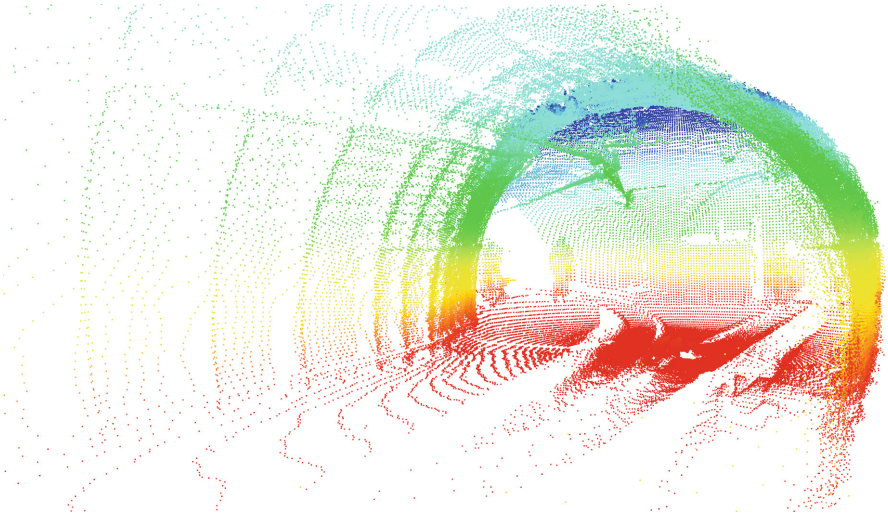

Fig. 21. Point cloud captured in coal mine Queen Luiza (Color figure online)

of a point cloud captured in the corridor shown in Fig. 20 is visible in Fig. 21. In this figure is visible Y-shaped juntion of corridors. The height of individual points is there differentiated by colour.

8 Conclusion

In this article was described the design of 3D LRF for the industrial environment. At first the dynamic analysis of the design was performed to properly select a rotatable actuator.

Then the arrangement of all parts, including a methane sensor, into the smallest volume was showed, followed by the design of the positioning unit housing. The diagram of control system showed complexity of this important part of 3D LRF. The surplus of computing power of the used main computer with 4 ARM cores is used for data preprocessing to simplify the subsequent point cloud processing in robotic systems. One welded stainless steel prototype was made and it was tested in real underground environment in a coal mine in Gliwice (Poland). In the end is presented an example of captured point cloud from this coal mine. The designed 3D LRF is working well and it is possible to use it on any robot in real industrial environment.

Acknowledgement. The project has been carried out in a framework of an EU programme of the Research fund for Coal and Steel under the grant agreement No. RFCR-CT-2014-00002 [14].

References

1. Bosse, M., Zlot, R., Flick, P.: Zebedee: design of a spring-mounted 3-D range sensor with application to mobile mapping. IEEE Trans. Robot. **28**(5), 1104–1119 (2012)
2. Zhang, J., Singh, S.: LOAM: lidar odometry and mapping in real-time. In: Robotics: Science and Systems Conference (RSS), pp. 109–111 (2014)
3. Cubero, S.: Industrial Robotics: Theory, Modelling and Control. Pro Literatur Verlag, Augsburg (2006). ISBN: 3866112858
4. Krumnikl, M., Olivka, P.: PWM nonlinearity reduction in microstep- ping unit firmware. Przegld Elektrotechniczny **88**(3a), 232–236 (2012)
5. Novák, P., Babjak, J., Kot, T., Olivka, P., Moczulski, W.: Exploration mobile robot for coal mines. In: Hodicky, J. (ed.) MESAS 2015. LNCS, vol. 9055, pp. 209–215. Springer, Heidelberg (2015)
6. Olivka, P., Krumnikl, M., Moravec, P., Seidl, D.: Calibration of short range 2D laser range finder for 3D SLAM usage. J. Sens. **501**, 3715129 (2016)
7. Kot, T., Krys, V., Mostyn, V., Novak, P.: Control system of a mobile robot manipulator. In: 2014 15th International Carpathian Control Conference (ICCC), pp. 258–263. IEEE (2014)
8. I Heart Robotics: More Hokuyo 3D Laser Scanner Images (2009). http://www.iheartrobotics.com/2009/06/more-hokuyo-3d-laser-scanner-images.html
9. Velodyne LiDAR, HDL-64E (2016). http://www.velodynelidar.com/
10. Sick, 2D Laser Scanner LMS111, Online Data Sheet. https://www.sick.com/media/pdf/2/42/842/dataSheet_LMS111-10100_1041114_en.pdf. Accessed 05 May 2016
11. Robotis, Servo Dynamixel MX-64R, e-Manual. http://support.robotis.com/en/product/dynamixel/mx_series/mx-64.htm. Accessed 10 May 2016
12. ZAM Service, Stationary Gas Detectors. http://www.zam-service.cz/www/index.php/en/produkty-3/detektory-plynu/stacionarni-detektory-zam
13. PTC Creo Parametric. http://www.ptc.com/cad/creo/parametric. Accessed 15 Apr 2016
14. TeleRescuer. http://www.telerescuer.eu/